ACS Macro Letters

Letter

pubs.acs.org/macroletters

Crystallization-Driven Thermoreversible Gelation of Coil-Crystalline Cyclic and Linear Diblock Copolypeptoids

Chang-Uk Lee,[†] Lu Lu,[†] Jihua Chen,[‡] Jayne C. Garno,[†] and Donghui Zhang*[,†]

[†]Department of Chemistry and Macromolecular Studies Group, Louisiana State University, Baton Rouge, Louisiana 70803, United States

[‡]Center for Nanophase Materials Sciences, Oak Ridge National Laboratory, Oak Ridge, Tennessee, Tennessee 37831, United States

Supporting Information

ABSTRACT: Methanol solutions of cyclic and linear coil-crystalline diblock copolypeptoids [i.e., poly(N-methyl-glycine)-*b*-poly(N-decyl-glycine)] (5−10 wt %) have been shown to form free-standing gels consisting of entangled fibrils at the room temperature. The gelation is thermally reversible and mechanically nonreversible. The gel-to-sol transition at the elevated temperature is induced by the melting of the PNDG crystalline domains which results in the morphological change of the fibrillar network into an isotropic solution. Variable-temperature NMR studies reveal that the cyclic polymer gels have higher gel-to-sol transition temperatures than the linear analogs. The hydrophobic segment is substantially less solvated in the cyclic polymers than the linear analogs both in gel and sol states. Rheological measurements reveal that the cyclic gels are stiffer than the linear counterparts, presumably due to the enhanced crystallinity in the fibrillar network in the formers relative to the latters. This study is the first example of thermoreversible gelation of coil-crystalline block copolymers, where the crystallization of the solvophobic segment has been shown to drive the gelation through the formation of crystalline fibrils.

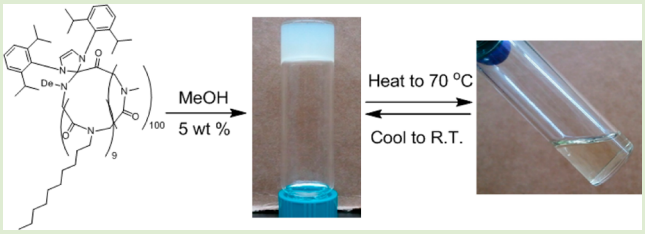

Hydrogels and organo-gels have attracted much attention in recent decades due to their wide use in various technical applications (e.g., coating, cosmetic and drug delivery). In contrast to chemical gels which consist of irreversibly cross-linked networks,[1] physical gels form networks that are reversibly cross-linked via interactions such as hydrophobic, hydrogen bonding, ionic/dative interactions or physical cross-linking.[2] As a result, physical gels can undergo sol−gel transition upon exposure to appropriate external stimuli, making them particularly attractive for applications where a nonpermanent network structure is desired.[3] While a variety of small organic molecules and polymers can induce physical gelation, polymer gels allow for convenient control over their morphology and mechanical properties through adjustment of the polymer composition, architecture, and concentration.

Block copolymers are known to self-assemble into micelles having various morphologies (e.g., spheres, discs, and worms) in dilute solution. Above a certain concentration and at a specific temperature, physical gelation can occur due to intermicellar interactions. Amphiphilic AB,[4] ABA,[5] or ABC[6] block copolymers have all been demonstrated to form gels due to the densification or cross-linking of spherical micelles through solvophilic blocks in concentrated solutions. In addition to being responsive toward temperature change, physical gels that respond to other environmental cues (e.g., pH,[7] light,[8] redox,[9] or chemical cues[10]) have also been developed through judicious design of the polymer structures.

Physical gelation due to the entanglement of fibrils (or worm micelles) is well-known for small organic gelators.[2] By contrast, reports on block copolymer gelators that operate by the same mechanism are limited.[11] This is due to the restricted window of access for polymeric worm micelles in the solution phase diagram, in contrast to spherical micelles or vesicles. One example is the core-cross-linked poly(ethylene oxide)-*b*-poly(butadiene) diblock copolymer (PEO-PB) that self-assembles into several micrometer-long worm micelles in water and forms a fragile gel at 1 wt % concentration.[12] Poly(ethylene oxide)−poly(propylene/butylene oxide)−poly(ethylene oxide) (PEO-PP/BO-PEO) forms a stiff gel at 40−52 wt % in water, and the gel structure is related to a mesophase involving hexagonal arrays of cylindrical micelles.[13,14] More recently, poly(glycerol monomethacrylate)-*b*-poly(2-hydroxypropyl methacrylate) (PGMA-*b*-PHPMA) diblock copolymers, directly synthesized in a 10 wt % aqueous solution, were shown to form a free-standing gel at 21 °C.[11] Cylindrical micelles were observed in the gel and transformed into spherical micelles upon cooling to 4 °C, resulting in the gel dissolution.

It has been shown recently that cylindrical micelles can be efficiently produced from the self-assembly of block copolymers containing an amorphous and a crystalline segment in dilute solution. Their formation is driven by the crystallization of

Received: December 28, 2012
Accepted: May 1, 2013
Published: May 3, 2013

core-forming segments.[15] Coil-crystalline diblock copolymers consisting of crystalline segments such as poly(PFDMS),[16] poly(ε-caprolactone),[17] poly(L-lactide),[18] polyethylene,[19] poly(3-hexylthiophene),[20] and poly(*N*-decyl glycine) (Figures S1–S4) have been reported.[21] However, physical gelation through entanglement or cross-linking of these cylindrical micelles has never been investigated. In this contribution, we demonstrate that a coil-crystalline diblock copolypeptoid [i.e., cyclic or linear poly(*N*-methyl glycine)-*b*-poly(*N*-decyl glycine) (*c*/*l*-PNMG$_{100}$-*b*-PNDG$_{10}$)] can form thermoreversible and mechanically nonreversible gels in methanol solution at 5–10 wt %. The gelation is driven by the crystallization of the solvophobic segments (PNDG) and the polymer architecture (i.e., cyclic vs linear) has been shown to affect the crystallization in the gel, gelation temperature and gel stiffness.

A cyclic poly(*N*-methyl glycine)-*b*-poly(*N*-decyl glycine) diblock copolymer was synthesized by *N*-heterocyclic carbene mediated zwitterionic polymerization of *N*-substituted *N*-carboxyanhydrides (i.e., Me-NCA and De-NCA) by sequential monomer addition (Scheme 1A). Their linear analog was

Scheme 1

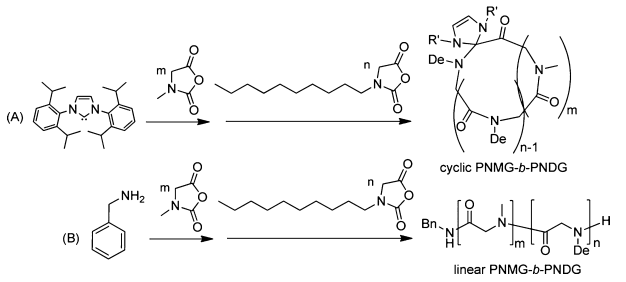

prepared by a similar polymerization method using a primary amine initiator (Scheme 1B). The polymers obtained from each reaction step have been confirmed by ^{1}H NMR spectroscopy and analyzed by size exclusion chromatography (SEC). The molecular parameters of the samples used in this study are shown in Table 1.

Cyclic and linear PNMG$_{100}$-*b*-PNDG$_{10}$ copolymers can be readily dissolved in methanol with slight heating. Cooling of a methanol solution containing 5 wt % or above of the cyclic polymers to room temperature results in the formation of opaque and free-standing gels (denoted as "cyclic gels") over a period of several hours. The gelation is thermally reversible: the gel dissolves into a clear and free-flowing liquid upon heating at ~70 °C (Figure S5). The linear polypeptoid analog undergoes a similar thermoreversible gelation, except that a higher concentration (>10 wt %) is required to form a free-standing gel (denoted as "linear gels"; Figure S5); the gelation of the linear polymer solutions also appears to be much slower than that of the cyclic analogs under identical conditions (refer to gel preparation in SI). The cyclic and linear polypeptoid free-standing gels are both mechanically nonreversible under high strain: vigorous shaking causes the gels to break up into smaller pieces and start to flow, suggesting the gel network is dynamically cross-linked. The gels are not restored upon prolonged equilibration.

Viscoelastic properties of the cyclic and linear gels were studied by rheological measurements at 25 °C. Analysis of the dynamic frequency sweep data in the linear viscoelastic regime (Figure 1) revealed a higher storage modulus (G') than the loss modulus (G'') in all concentration ranges (2, 5, and 10 wt %) for the cyclic gels, indicative of a highly elastic response. G' and G'' were found to increase gradually with increasing frequency over a range of three decades (10^{-1}–10^{2} rad·s^{-1}), suggesting an enhanced elastic response at higher frequency and the structural relaxation at lower frequency. For a permanent network with infinite relaxation time, G' and G'' are expected to be independent of the deformation frequency. Clearly, the polypeptoid gels consist of highly dynamic networks where the structural relaxation occurs on the experimental time scale. Similar behaviors have been previously reported for gels based on colloidal particles where high deformation frequency induces an elastic response from the local structures, which can relax on a longer time scale.[22−24] As the concentration of the cyclic polypeptoid gel increases from 2 to 5 wt %, the storage moduli of the gels (G' and G'') dramatically increases by 2 orders of magnitude, indicating a change from a soft to a hard gel. The G' and G'' of 5 and 10 wt % gels are comparable in all frequency ranges, suggesting similar stiffness of the two gels. The linear gels exhibit similar responses as the cyclic analogs in the dynamic frequency sweep measurement. Interestingly, the G' and G'' of the linear gels are lower than those of their cyclic analogs (Figure S6). For example, at the 10 rad·s^{-1} frequency, the G' of the 5 wt % cyclic gel is 20-fold

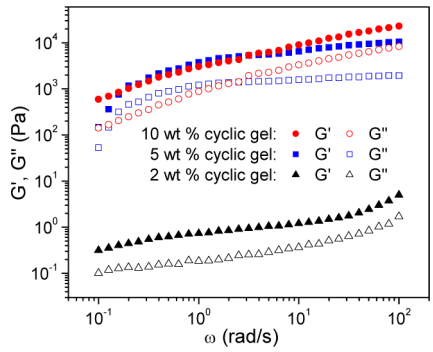

Figure 1. Storage modulus (G') and loss modulus (G'') of cyclic PNMG$_{100}$-*b*-PNDG$_{10}$ gels in methanol (2, 5, or 10 wt %) as a function of angular frequency (ω) at a strain amplitude of γ = 1.0% at 25 °C.

Table 1. Molecular Parameters of *c*/*l*-PNMG-*b*-PNDG Diblock Copolymers

sample[a]	N_{PNMG}[b]	N_{PNDG}[c]	M_n[d] (kD)	M_n[e] (kD)	PDI[e]	f_{PNDG}[f]
c-PNMG$_{100}$-*b*-PNDG$_{10}$	100	10	9.5	14.7	1.21	0.09
l-PNMG$_{100}$-*b*-PNDG$_{10}$	100	10	9.2	12.5	1.05	0.09

[a]The numbers in subscripts correspond to number average degree of polymerization (DP), as determined by ^{1}H NMR spectroscopy. [b]The DP of the PNMG blocks was determined by end-group analysis using ^{1}H NMR spectroscopy in CD_3OD. [c]The DP of PNDG blocks relative to that of PNMG was determined by ^{1}H NMR spectroscopy in $CDCl_3/CF_3CO_2D$. [d]The number average molecular weights were calculated using the polymer composition determined by ^{1}H NMR spectroscopy. [e]The relative number average molecular weights and polydispersity index were determined by size exclusion chromatography using polystyrene standards in DMF/LiBr(0.01 M). [f]The molar fraction of the PNDG blocks was calculated using the polymer composition determined by ^{1}H NMR spectroscopy.

dx.doi.org/10.1021/mz300667n | ACS Macro Lett. 2013, 2, 436–440

larger than that of the linear counterpart, indicating the former gel is harder than the latter (Figure S6A).

The elastic gel-like behavior is also reflected by the presence of an apparent yield stress for both the cyclic and the linear gels (Figure S7A). The yield stress refers to the applied stress above which the gel ruptures or starts to flow. The yield stress was estimated from the dynamic strain sweep measurements where the elastic stress (σ) is obtained from $\sigma = G'\gamma$ (G', storage modulus; γ, strain, Figure S7B). The yield stress of the 5 wt % cyclic gel is 198 (5) Pa, whereas that of the linear gel is much lower at 7 (1) Pa. This is consistent with the results from the dynamic frequency sweep experiments and our empirical observation that the cyclic gels are harder than the linear analogs under identical conditions. Steady shear experiments were conducted to probe the mechanically nonreversible characteristics of the gels. It is evident that both the cyclic and linear gels thin dramatically above a specific stress threshold (Figure S7A), as evidenced by the apparent viscosity decreases with increasing shear rate above the yield stress threshold (Figure S8). The gel structures were not restored after extended equilibration time, consistent with mechanically nonreversible gels.

Entangled fibrillar structures measuring micrometer lengths are evident in the AFM images of Figure 2. The individual fibril

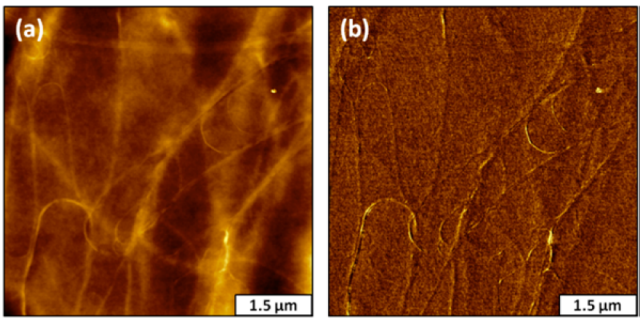

Figure 2. Fibrillar structures of the linear $PNMG_{100}$-*b*-$PNDG_{10}$ gel (5 wt % in methanol) acquired by tapping-mode AFM: (a) topograph, 6 × 6 μm^2 view; (b) corresponding phase image.

has a diameter measuring 31 ± 6 nm for both the cyclic and the linear gel samples (Figures S9 and S10). The fibrils are twisted or aligned side by side to form bundles of varying diameters. For the cyclic and linear gels, the average bundle diameters measured 56 ± 12 and 120 ± 56 nm, whereas the bundle heights are 6.5 ± 2.9 and 3.2 ± 1.1 nm, respectively. The cyclic gel appears to contain a substantially higher density of bundles than the analogous linear gel with identical polymer concentration.

To obtain additional structural information, the cyclic and linear free-standing gels (10 wt %) were analyzed by small/wide-angle X-ray scattering techniques (S/WAXS). Both samples exhibit two notable peaks at q = 0.26 and 0.089 $Å^{-1}$ in the WAXS diffractograms (Figure 3A). The former peak (d = 24 Å) corresponds to the interchain crystalline packing of the PNDG segments in the crystalline domain.[21] This peak is stronger for the cyclic gel than the linear one, indicating enhanced crystalline packing of the former relative to the latter. The low q peak corresponds to a domain spacing of 7 nm, which is smaller than the PNDG crystalline core diameter of the individual cylindrical micelle (~12 nm) observed by cryoTEM in the dilute solution (Figures S1 and S2).[21] The

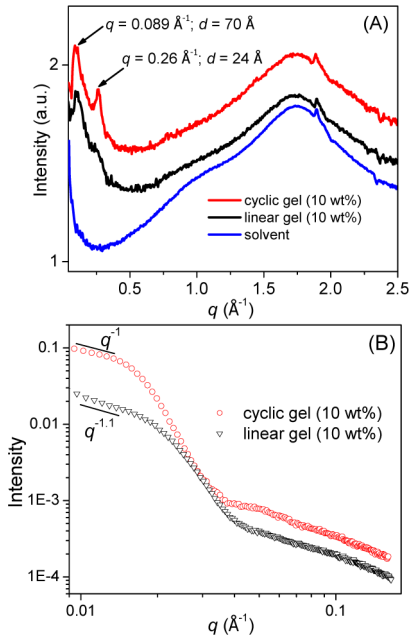

Figure 3. (A) WAXS and (B) SAXS diffractograms of the cyclic and linear $PNMG_{100}$-*b*-$PNDG_{10}$ free-standing gels (10 wt % in methanol) obtained after 20 h gelation at room temperature.

peak intensity is comparable between the cyclic and the linear gel. The origin of this peak is currently unclear and warrants further investigation. SAXS analysis revealed that both gels asymptoted to a slope of −1 on the log−log plot in the low q region, indicative of $I \sim q^{-1}$ scaling expected for long cylindrical particles (Figure 3B).[11] Thus, the SAXS data is consistent with the observation of fibrils by AFM. Analysis of the low q data by the Guinier plot, that is, $\ln[I(q) \times q]$ versus q^2 allows for the extraction of the cylinder's diameter: d = 28 ± 3 and 20 ± 2 nm for the cyclic and linear gels, respectively (Figure S11). These values agree reasonably with the fibril diameter determined by the AFM analysis. The cyclic gel scatters more intensely in the low q region than the linear analog, which results from a higher number density of cylindrical scatterers in the former than the latter.[11]

Thermoreversible gelation of the cyclic $PNMG_{100}$-*b*-$PNDG_{10}$ in methanol (10 wt %) was also investigated by differential scanning calorimetry (DSC; Figure S12). As the sample was heated from 10 to 65 °C, a broad endothermic first-order transition was observed at 55 °C (transition window ΔT= 15 °C) with a 15.8 ± 0.5 $J \cdot g^{-1}$ enthalpic change (ΔH_m). The gel-to-sol transition coincides with the melting of the crystalline PNDG domain in the cylindrical micelles of the same block copolypeptoid in dilute methanol solution (Figure S2).[21] In the cooling cycle (cooling rate = 2.0 $°C \cdot min^{-1}$), no crystallization exotherms were observed, suggesting that prolonged time is required for the crystallization of the PNDG segments and subsequent gelation. The mass of the gels remain unchanged before and after the DSC experiment, suggesting that the endothermic peak did not result from solvent evaporation. By contrast, no notable thermal transition was observed for the analogous linear gel in both the heating and the cooling cycles, consistent with the low crystallinity in the linear gel relative to the cyclic gel.

Polarized optical microscopic (POM) analysis of the cyclic gel (Figure S13) at room temperature revealed the presence of birefringent domains in micrometer size that disappeared upon

dx.doi.org/10.1021/mz300667n | ACS Macro Lett. 2013, 2, 436−440

heating to 60 °C, at which the gel became an isotropic free-flowing liquid. The birefringent domains reformed upon cooling from 60 °C to room temperature, which preceded the formation of a free-standing gel. They are likely to form from the extensive bundling of the long fibrils. By comparison, birefringent domains were much more sparsely observed in the analogous linear gel than the cyclic one. The POM results are consistent with the time-lapsed WAXS analysis of the gelation where the crystallization was also found to occur before the macroscopic gelation and the crystallinity in the gels increased with the gelation time (Figure S14). These results strongly suggest that the gelation of *c*-PNMG$_{100}$-*b*-PNDG$_{10}$ in methanol is driven by the crystallization of the PNDG segments in the block copolypeptoids.

Variable temperature ^{1}H NMR studies were conducted for the 5 wt % cyclic and linear gels between 10 and 65 °C to gain insights into temperature-induced change of solvation around the polymers and the solution morphology (Figure 4). Plot of

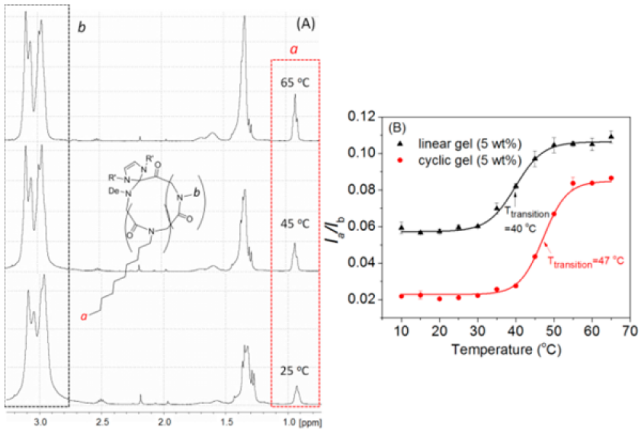

Figure 4. (A) ^{1}H NMR spectra of the cyclic PNMG$_{100}$-*b*-PNDG$_{10}$ gel in CD_3OD (5 wt %) at 25, 45, and 65 °C; (B) the integration ratio of the PNDG methyl protons to the PNMG methyl protons in the cyclic (●) and the linear PNMG$_{100}$-*b*-PNDG$_{10}$ gels (5 wt %; ▲) as different temperatures, and their respective sigmoidal fitting.

the integration ratio of PNDG methyl protons (*a*) relative to that of PNMG (*b*) as a function of temperature reveals a two-state transition, in accord with a gel-to-sol transition with increasing temperature for both samples. Sigmoidal fitting of the curve gives the transition temperature at 47 and 40 °C and transition windows of 14 and 16 °C for the cyclic and linear gels, respectively (Figure 4). For both gels, the integration ratio is higher at high temperature state (sol state) than that at the low temperature state (gel state), suggesting enhanced solvation and mobility of the solvophobic PNDG segments in the former relative to the latter. Interestingly, in both the sol and the gel states, the integration ratios for the linear gel are higher than those for the cyclic counterpart. This suggests that the PNDG segments are more solvated in the linear sample than the cyclic analog in both the gel and the sol states. In the gel state, this can be understood by the enhanced crystallinity in the PNDG segments in the fibrils of the cyclic gel relative to the linear one, resulting in reduced chain mobility and solvation in the former relative to the latter. In the sol state where the nonassociated polymers dominate as evidenced by the DLS analysis (Figure S3), the cyclic polymer chains are in a more collapsed conformation relative to the linear analogs, contributing to the reduced solvation of the PNDG segment in the former relative to the latter.

In conclusion, we have demonstrated that the coil-crystalline diblock copolypeptoids can efficiently form thermoreversible free-standing gels at moderate concentrations (5−10 wt %) in methanol at room temperature. The gels consist of a network of crystalline fibrils cross-linked by dynamic entanglement. Rheological studies revealed that cyclic copolypeptoids produced stiffer gels than the linear counterparts. This is partially ascribed to the difference in the degree of crystalline packing of the PNDG segments in the fibrils, resulting in enhanced rigidity for the fibrils and crystalline cross-linking sites for the cyclic gels than the linear analogs. This study is the first example of thermoreversible gelation of coil-crystalline block copolymers where the crystallization of the solvopohobic segments has been shown to drive the gelation through the formation of the crystalline fibrils.

■ ASSOCIATED CONTENT

Supporting Information

Experimental procedures; optical images showing thermoresponsive gelation from *c*/*l*-PNMG$_{100}$-*b*-PNDG$_{10}$ diblock copolymers in methanol; selected area electron diffraction (SAED), microcalorimetric, DLS, and ^{1}H NMR analysis of spherical and cylindrical micelles of *c*-PNMG$_{100}$-*b*-PNDG$_{10}$ in dilute methanol solution; dynamic and steady-state rheological measurements of the cyclic and linear gels; DSC thermograms and POM images of the cyclic gel; full ^{1}H NMR spectra of *c*/*l*-PNMG$_{100}$-*b*-PNDG$_{10}$ at different temperature; the Guinier plot of SAXS data for the cyclic and linear gel; time-lapsed WAXS data of the cyclic and linear gel; AFM images of cyclic and linear gels. This material is available free of charge via the Internet at http://pubs.acs.org.

■ AUTHOR INFORMATION

Corresponding Author

*E-mail: dhzhang@lsu.edu.

Notes

The authors declare no competing financial interest.

■ ACKNOWLEDGMENTS

The authors thank Dr. Vince J. LiCata for providing access to the VP-DSC. The authors also thank Dr. Qinglin Wu for providing access to the rheometer. A portion of this research was conducted at the Center for Nanophase Materials Sciences, which is sponsored at Oak Ridge National Laboratory by the Scientific User Facilities Division, Office of Basic Energy Sciences, U.S. Department of Energy. This work is supported by the National Science Foundation (CHE0955820 and CHE0847291), NASA, and the Louisiana Board of Regents [NASA/LEQSF(2011-14)-Phase3-05]. J.C.G. also acknowledges the Camille Dreyfus Teacher-Scholar program and the Petroleum Research Fund New Directions program.

■ REFERENCES

(1) Appel, E. A.; del Barrio, J.; Loh, X. J.; Scherman, O. A. *Chem. Soc. Rev.* **2012**, *41*, 6195−6214.
(2) Buerkle, L. E.; Rowan, S. J. *Chem. Soc. Rev.* **2012**, *41*, 6089−6102.
(3) Huynh, C. T.; Nguyen, M. K.; Lee, D. S. *Macromolecules* **2011**, *44*, 6629−6636.
(4) Li, H.; Yu, G.-E.; Price, C.; Booth, C.; Hecht, E.; Hoffmann, H. *Macromolecules* **1997**, *30*, 1347−1354.

(5) Jeong, B.; Bae, Y. H.; Lee, D. S.; Kim, S. W. *Nature* **1997**, *388*, 860−862.
(6) Zhou, C.; Hillmyer, M. A.; Lodge, T. P. *J. Am. Chem. Soc.* **2012**, *134*, 10365−10368.
(7) Nguyen, M. K.; Park, D. K.; Lee, D. S. *Biomacromolecules* **2009**, *10*, 728−731.
(8) Jiang, X.; Jin, S.; Zhong, Q.; Dadmun, M. D.; Zhao, B. *Macromolecules* **2009**, *42*, 8468−8476.
(9) Li, C.; Madsen, J.; Armes, S. P.; Lewis, A. L. *Angew. Chem., Int. Ed.* **2006**, *45*, 3510−3513.
(10) Han, D.; Boissiere, O.; Kumar, S.; Tong, X.; Tremblay, L.; Zhao, Y. *Macromolecules* **2012**, *45*, 7440−7445.
(11) Blanazs, A.; Verber, R.; Mykhaylyk, O. O.; Ryan, A. J.; Heath, J. Z.; Douglas, C. W. I.; Armes, S. P. *J. Am. Chem. Soc.* **2012**, *134*, 9741−9748.
(12) Won, Y. Y.; Davis, H. T.; Bates, F. S. *Science* **1999**, *283*, 960−963.
(13) Mortensen, K.; Pedersen, J. S. *Macromolecules* **1993**, *26*, 805−812.
(14) Waton, G.; Michels, B.; Steyer, A.; Schosseler, F. *Macromolecules* **2004**, *37*, 2313−2321.
(15) Gilroy, J. B.; Rupar, P. A.; Whittell, G. R.; Chabanne, L.; Terrill, N. J.; Winnik, M. A.; Manners, I.; Richardson, R. M. *J. Am. Chem. Soc.* **2011**, *133*, 17056−17062.
(16) Wang, X.; Guerin, G.; Wang, H.; Wang, Y.; Manners, I.; Winnik, M. *Science* **2007**, *317*, 644.
(17) Du, Z.-X.; Xu, J.-T.; Fan, Z.-Q. *Macromolecules* **2007**, *40*, 7633−7637.
(18) Petzetakis, N.; Walker, D.; Dove, A. P.; O'Reilly, R. K. *Soft Matter* **2012**, *8*, 7408−7414.
(19) Schmalz, H.; Schmelz, J.; Drechsler, M.; Yuan, J.; Walther, A.; Schweimer, K.; Mihut, A. M. *Macromolecules* **2008**, *41*, 3235−3242.
(20) Gilroy, J. B.; Lunn, D. J.; Patra, S. K.; Whittell, G. R.; Winnik, M. A.; Manners, I. *Macromolecules* **2012**, *45*, 5806−5815.
(21) Lee, C. U.; Smart, T. P.; Guo, L.; Epps, T. H., III; Zhang, D. *Macromolecules* **2011**, *44*, 9574−9585.
(22) Trappe, V.; Weitz, D. A. *Phys. Rev. Lett.* **2000**, *85*, 449−452.
(23) Weng, W.; Beck, J. B.; Jamieson, A. M.; Rowan, S. J. *J. Am. Chem. Soc.* **2006**, *128*, 11663−11672.
(24) Yang, M. C.; Scriven, L.; Macosko, C. *J. Rheol.* **1986**, *30*, 1015−1029.